Approximate theory of reverberation in rectangular rooms with specular and diffuse reflections

Tetsuya Sakuma[a)]
Graduate School of Frontier Sciences, The University of Tokyo, 5-1-5 Kashiwanoha, Kashiwa, Chiba 277-8563, Japan

(Received 22 August 2011; revised 26 July 2012; accepted 26 July 2012)

First, an approximate theory of reverberation in rectangular rooms is formulated as a specular reflection field based on the image source method. In the formulation, image sources are divided into axial, tangential, and oblique groups, which chiefly contribute to the corresponding groups of normal modes in wave acoustics. Consequently, the total energy decay consists of seven kinds of exponential decay curves. Second, considering surface scattering on walls with scattering coefficients, an integrated reverberation theory for nondiffuse field is developed, where the total field is divided into specular and diffuse reflection fields. The specular reflection field is simply formulated by substituting *specular* absorption coefficients, while the diffuse reflection field is assumed to be a perfectly diffuse field, of which energy is supplied from the specular reflection field at each reflection. Finally, a theoretical case study demonstrates how surface scattering affects the energy decay in rectangular rooms with changing the aspect ratio and the absorption distribution. © *2012 Acoustical Society of America*. [http://dx.doi.org/10.1121/1.4747001]

PACS number(s): 43.55.Br, 43.20.Fn [LMW] Pages: 2325–2336

I. INTRODUCTION

In the field of room acoustics, reverberation is one of the most important aspects for judging acoustical qualities of every kind of room, thus it is to be quantified, predicted, and controlled. For this reason, a variety of theories of reverberation in rooms have been proposed, originated from Sabine's formula[1] on the assumption of perfectly diffuse field, modified by Eyring,[2] Norris,[3] Millington,[4] Sette,[5] Kuttruff,[6,7] and others. The first two classical formulas are still widely used for room acoustics design, although they cannot take into account room shapes and absorption distribution.[8] Actually, the classical formulas often underestimate the reverberation time of usual rooms, most of which have rectangular shapes and nonuniform absorption distribution.

For rectangular rooms, an empirical formula was first proposed by Fitzroy,[9] and followed by Pujolle,[10] Hirata,[11] Arau-Puchades,[12] Nilsson,[13], Neubauer,[14] and others. Fitzroy's formula empirically assumes the arithmetic mean of reverberation times of the three orthogonal directions, while Arau-Puchades's formula assumes the geometric mean with a theoretical consideration. Both of the formulas are simple to calculate, but do not work adequately in various situations. Hirata derived a reverberation theory based on the image source method, decomposing the sound field into one-, two-, and three-dimensional fields with frequency dependence. At first sight, this approach seems to correspond to the normal mode theory based on wave acoustics; however, some discrepancy is seen due to a misunderstanding in the theoretical development.

Generally, surface scattering tends to heighten field diffuseness, resulting in a decrease in reverberation time, but the effect strongly depends on room shapes and absorption distribution.[15–17] In a room with regular shape and nonuniform absorption, the effect of surface scattering can be great, and conversely, with irregular shape and uniform absorption, it can be small or negligible. Recently, as a measure of the efficiency of surface scattering, the scattering coefficient has been widely used for geometric acoustic simulation.[18] Its measurement method was already standardized in ISO 17497-1,[19] and computational methods are also available for predicting it.[20,21] However, up to now there exists no reverberation theory including the scattering coefficient, which must be based on some theory for nondiffuse field, although some research has been concerned with sound fields including both specular and diffuse reflections.[22–24]

In this paper, first, an approximate theory of reverberation in rectangular rooms is formulated as a specular reflection field based on the image source method by modifying Hirata's theory. Second, considering surface scattering on walls with scattering coefficients, an integrated reverberation theory for nondiffuse field is developed, where the total field is divided into specular and diffuse reflection fields. Finally, a theoretical case study is presented to demonstrate how surface scattering affects the energy decay of nondiffuse fields in rectangular rooms, with changing the aspect ratio and the absorption distribution.

II. REVERBERATION OF SPECULAR REFLECTION FIELD IN RECTANGULAR ROOMS

A. Specular field of image sources

As illustrated in Fig. 1, a regular arrangement of image sources is determined for a point source in a rectangular room. When the energy density of the reflection field is discussed with space average for both source and receiver, a continuous distribution of image sources is considered with

[a)]Author to whom correspondence should be addressed. Electronic mail: sakuma@k.u-tokyo.ac.jp

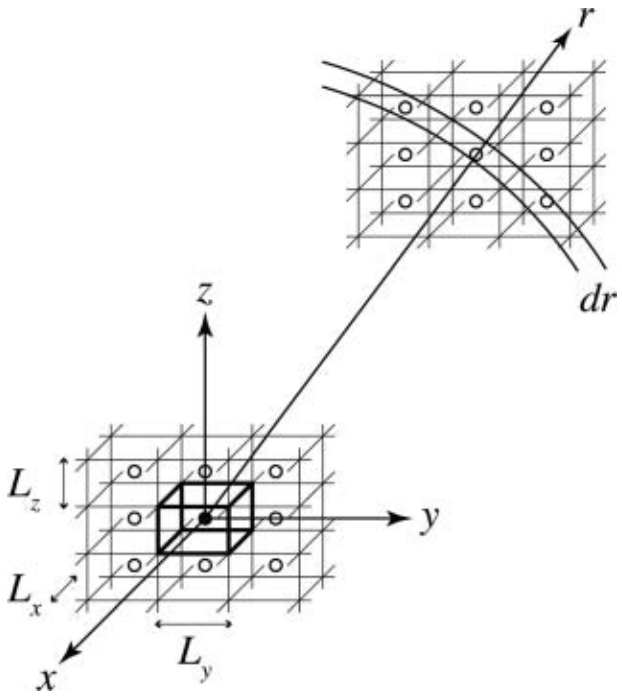

FIG. 1. Image sources of a rectangular room.

a representative receiving point at the center of the room. For image sources at equal distances from the receiving point, the number of sources, distance attenuation, and wall absorption are estimated on the condition that only specular reflections occur throughout the paths. If the real source of the sound power W is stopped at $t=0$ in the steady state, the average energy density of the three-dimensional specular field is formulated in spherical coordinates, as follows ($t \geq 0$):

$$E^{\mathrm{S}}(t) = \int_0^{2\pi}\int_0^{\pi}\int_{ct}^{\infty} \frac{W}{4\pi c r^2}(1-\tilde{\alpha}_x)^{r\sin\theta\cos\varphi/L_x} \times (1-\tilde{\alpha}_y)^{r\sin\theta\sin\varphi/L_y}(1-\tilde{\alpha}_z)^{r\cos\theta/L_z}\frac{r^2\sin\theta dr d\theta d\varphi}{L_x L_y L_z}, \tag{1}$$

where c is the sound speed, $L_{x(y,z)}$ is the length of each side, and $\tilde{\alpha}_{x(y,z)}$ is the absorption coefficient averaged by the geometric mean of two reflection coefficients in each direction. Because of alternate reflections between the parallel surfaces, the geometric average is used, represented by

$$\tilde{\alpha}_{x(y,z)} = 1 - \sqrt{\left(1-\alpha^{+}_{x(y,z)}\right)\left(1-\alpha^{-}_{x(y,z)}\right)}, \tag{2}$$

where $\alpha^{\pm}_{x(y,z)}$ are the absorption coefficients of two parallel walls. Generally, Eq. (1) is composed of direction-dependent multiple exponentials, and numerical integration is required to evaluate the exact energy decay.[8]

In a similar way to the classical reverberation theory, a single exponential decay function is roughly assumed, where the mean free path for oblique sources l_{ob} is approximately equal to the theoretical value for the three-dimensional perfectly diffuse field $l_{\mathrm{r}} = 4V/S$ (see the first section of the Appendix),[25] with the room volume $V = L_x L_y L_z$, and the total surface area $S = 2(L_x L_y + L_y L_z + L_z L_x)$. Furthermore, the area-weighted arithmetic mean of absorption coefficients for the three directions is used as represented by

$$\alpha_{\mathrm{ob}} = \frac{L_y L_z \tilde{\alpha}^{\mathrm{r}}_x + L_z L_x \tilde{\alpha}^{\mathrm{r}}_y + L_x L_y \tilde{\alpha}^{\mathrm{r}}_z}{L_y L_z + L_z L_x + L_x L_y}, \tag{3}$$

where $\tilde{\alpha}^{\mathrm{r}}_{x(y,z)}$ is the geometric mean of random-incidence absorption coefficients in each direction according to Eq. (2). Consequently, Eq. (1) is approximated by

$$E^{\mathrm{S}}_{\mathrm{ob}}(t) = \int_{ct}^{\infty} \frac{W}{4\pi c r^2}(1-\alpha_{\mathrm{ob}})^{r/l_{\mathrm{ob}}}\frac{4\pi^2 dr}{V} = \frac{W}{c\hat{A}_{\mathrm{ob}}}\exp\left(-\frac{c\hat{A}_{\mathrm{ob}}}{V}t\right), \tag{4}$$

with $\hat{A}_{\mathrm{ob}} = A_{\mathrm{ob}}/4$, $A_{\mathrm{ob}} = S\alpha_{\mathrm{Eob}}$ and $\alpha_{\mathrm{Eob}} = -\ln(1-\alpha_{\mathrm{ob}})$. For a general expression, the quantity $\hat{A}$ is defined as the room absorption factor taking into account the ratio of incident intensity to energy density, thus giving $\hat{A}/V = \alpha_{\mathrm{E}}/l$ throughout this paper.

Equation (4) is regarded as a first approximation for the specular field of oblique sources, in a similar form to Eyring's formula using Millington's average absorption coefficient for each pair of parallel walls. However, it includes the contributions of axial and tangential sources that are more apt to deviate from the average decay. In the following, one-, two-, and three-dimensional specular fields are considered by dividing image sources into axial, tangential, and oblique groups, which chiefly contribute to the corresponding groups of normal modes in wave acoustics.

B. Specular fields of axial sources

Consider the image sources near the x axis in the angular ranges within $\pm\theta_y$ and within $\pm\theta_z$ to the positive and negative x directions, as illustrated in Fig. 2. The x-axial sources lead to normal incidence to the x-directional walls (in yz plane), and grazing incidence to the y- and z-directional walls. If the off-axial path differences from an x-axial source to the room in y and z directions are, respectively, within 1/4 wavelength ($\pi/2$ in phase), the image source chiefly contributes to x-axial modes in wave acoustics. For far x-axial sources at small angles of $\theta_{y(z)}$, the maximum path differences are expressed by $\Delta_{y(z)} \approx L_{y(z)} \sin\theta_{y(z)} \approx L_{y(z)}\theta_{y(z)}$, thus the critical angles are generally defined as

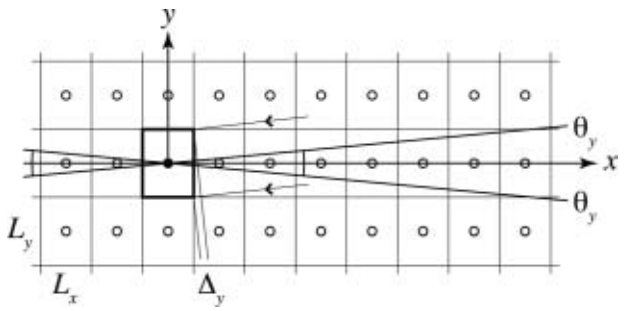

FIG. 2. Axial image sources for the x axis in the xy plane.

$$\theta_{x(y,z)} = \frac{\pi c}{2\omega L_{x(y,z)}}, \tag{5}$$

with the angular frequency ω.

At the critical angles $\theta_{y(z)}$, the frequency of normal reflections on the x-directional walls is expressed by $n_{ax} \approx c/L_x$, and those of grazing reflections on the y- and z-directional walls by $n_{axy(z)} = c \sin\theta_{y(z)}/L_{y(z)} \approx c\theta_{y(z)}/L_{y(z)}$. In the angular ranges, the average reflection frequency for the x direction, $\bar{n}_{ax} \approx n_{ax}$, and those for the y and z directions, $\bar{n}_{axy(z)} \approx n_{axy(z)}/2$. By limiting the angular ranges of integration in Eq. (1), the energy density of the one-dimensional specular field from x-axial sources is formulated as follows:

$$\begin{aligned} E^{\mathrm{S}}_{ax}(t) &= \frac{4W}{c}\int_{ct}^{\infty}(1-\tilde{\alpha}^{\mathrm{n}}_x)^{r/L_x}(1-\tilde{\alpha}^{\mathrm{g}}_y)^{r\theta_y/2L_y} \\ &\quad\times(1-\tilde{\alpha}^{\mathrm{g}}_z)^{r\theta_z/2L_z}\frac{2(2\theta_y)(2\theta_z)dr}{4\pi} \\ &= \frac{4W}{c}\frac{\pi c^2 L_x}{2\omega^2 V^2}\int_{ct}^{\infty}(1-\alpha_{ax})^{r/l_x}dr \\ &= \frac{4W}{c}\frac{\pi c^2 L_x}{2\omega^2 V\hat{A}_{ax}}\exp\left(-\frac{c\hat{A}_{ax}}{V}t\right) \end{aligned} \tag{6}$$

where the one-dimensional mean free path $l_x = L_x$, and the contribution of axial sources to the one-dimensional field is assumed quadruple to that of oblique sources to the three-dimensional field due to the coherence in the two off-axial directions, in accordance with the ratio of normalization factors in the mode theory. Regarding wall absorption,

$$\begin{aligned} &\hat{A}_{ax} = 2A_{ax},\ \ A_{ax} = 2L_yL_z\alpha_{Eax},\ \ \alpha_{Eax} = -\ln(1-\alpha_{ax}), \\ &\alpha_{ax} = 1-(1-\tilde{\alpha}^{\mathrm{n}}_x)(1-\tilde{\alpha}^{\mathrm{g}}_y)^{\varepsilon_{axy}}(1-\tilde{\alpha}^{\mathrm{g}}_z)^{\varepsilon_{axz}}, \end{aligned} \tag{7}$$

$$\varepsilon_{axy(z)} = \frac{\bar{n}_{axy(z)}}{\bar{n}_{ax}} \approx \frac{\pi c L_x}{4\omega L^2_{y(z)}}, \tag{8}$$

where $\tilde{\alpha}^{\mathrm{n}}_x$ is the normal-incidence absorption coefficient of the x-directional walls, and $\tilde{\alpha}^{\mathrm{g}}_{y(z)}$ are the grazing-incidence absorption coefficients of the y- and z-directional walls, considered as the geometric mean for parallel walls according to Eq. (2). In the strict sense, the above-presented normal and grazing incidence correspond to incidence from the angular ranges of axial sources with frequency dependence; accordingly, a database of directional absorption coefficients is needed. Practically, rough estimates of the normal- and grazing-incidence coefficients are available on the assumption of local reaction (see the second section of the Appendix). The total average absorption coefficient for the one-dimensional field, α_{ax}, is given by taking into account the reflection frequency in each direction, with $\varepsilon_{axy(z)}$ the ratios of average reflection frequency of the y and z to the x direction.

In Eq. (7), the geometric mean weighted with average reflection frequency is given, for the reason that the reflection frequency in each direction is almost independent for axial sources. However, it is not valid for an extreme case in which that either grazing-incidence absorption coefficient $\tilde{\alpha}^{\mathrm{g}}_{y(z)} = 1$, because the contribution of x-axial sources perfectly vanishes in Eq. (6), even if one of the y- and z-directional walls has perfect absorption.

C. Specular fields of tangential sources

In a similar way to axial sources, consider the image sources near the xy plane in the angular range within $\pm\theta_z$ to the xy plane, which lead to random incidence to the x- and y-directional walls, and grazing incidence to the z-directional walls (in xy plane). Again, if the off-tangential path difference from an xy-tangential source to the room in z direction is within 1/4 wavelength ($\pi/2$ in phase), the image source chiefly contributes to the xy-tangential modes. Thus, the critical angles by Eq. (5) are in common with axial and tangential sources.

In the angular range, the average frequency of reflections for the x- and y-directional walls is $\bar{n}_{txy} \approx c/l_{xy}$, with the two-dimensional mean free path $l_{xy} = \pi L_xL_y/2(L_x + L_y)$ (see the first section of the Appendix), and the average frequency of grazing reflections for the z-directional walls, $\bar{n}_{tz} \approx n_{tz}/2 \approx c\theta_z/2L_z$. Similar to Eq. (6), the energy density of the two-dimensional specular field from xy-tangential sources is formulated as follows:

$$\begin{aligned} E^{\mathrm{S}}_{txy}(t) &= \frac{2W}{c}\int_{ct}^{\infty}(1-\tilde{\alpha}^{\mathrm{r}}_{xy})^{r/l_{xy}}(1-\tilde{\alpha}^{\mathrm{g}}_z)^{r\theta_z/2L_z}\frac{2\pi(2\theta_z)dr}{4\pi V} \\ &= \frac{2W}{c}\frac{\pi c L_xL_y}{2\omega V^2}\int_{ct}^{\infty}(1-\alpha_{txy})^{r/l_{xy}}dr \\ &= \frac{2W}{c}\frac{\pi c L_xL_y}{2\omega V\hat{A}_{txy}}\exp\left(-\frac{c\hat{A}_{txy}}{V}t\right), \end{aligned} \tag{9}$$

where the contribution of tangential sources to the two-dimensional field is assumed double that of oblique sources to the three-dimensional field due to the coherence in the off-tangential direction. Regarding wall absorption, $\hat{A}_{txy} = A_{txy}/\pi$, $A_{txy} = 2(L_x + L_y)L_z\alpha_{Etxy}$, $\alpha_{Etxy} = -\ln(1-\alpha_{txy})$,

$$\alpha_{txy} = 1-(1-\tilde{\alpha}^{\mathrm{r}}_{xy})(1-\tilde{\alpha}^{\mathrm{g}}_z)^{\varepsilon_{tz}}, \tag{10}$$

$$\tilde{\alpha}^{\mathrm{r}}_{xy} = \frac{L_y\tilde{\alpha}^{\mathrm{r}}_x + L_x\tilde{\alpha}^{\mathrm{r}}_y}{L_y + L_x}, \tag{11}$$

$$\varepsilon_{tz} = \frac{\bar{n}_{tz}}{\bar{n}_{txy}} \approx \frac{\pi^2 c L_xL_y}{8\omega(L_x + L_y)L_z^2}, \tag{12}$$

where $\tilde{\alpha}^{\mathrm{r}}_{xy}$ is the area-weighted arithmetic mean of random-incidence values for the two directions, considering alternate reflections by Eq. (2), and α_{txy} is the total average absorption coefficient for the two-dimensional field, with ε_{tz} the ratio of average reflection frequency of the z direction to the x and y directions. Note that Eq. (10) is again not valid if one of the z-directional walls has perfect absorption yielding $\tilde{\alpha}^{\mathrm{g}}_z = 1$, because the contribution of xy-tangential sources perfectly vanishes in Eq. (9).

D. Reverberation of total specular field

Equation (1) includes the contributions of axial and tangential sources, and Eq. (9) also includes that of axial sources. Summing up Eqs. (1), (6), and (9), excluding the

above-presented duplicate contributions, the total energy density of specular fields in the room is expressed by

$$E^{\mathrm{S}}(t) = \frac{W}{c}\left[\frac{\gamma_{\mathrm{ob}}}{\hat{A}_{\mathrm{ob}}}\exp\left(-\frac{c\hat{A}_{\mathrm{ob}}}{V}t\right) + \sum_{xy}\frac{2\gamma_{\mathrm{t}xy}}{\hat{A}_{\mathrm{t}xy}}\exp\left(-\frac{c\hat{A}_{\mathrm{t}xy}}{V}t\right) + \sum_{x}\frac{4\gamma_{\mathrm{a}x}}{\hat{A}_{\mathrm{a}x}}\exp\left(-\frac{c\hat{A}_{\mathrm{a}x}}{V}t\right)\right], \tag{13}$$

where the proportion of sources in each group is denoted by

$$\gamma_{\mathrm{ob}} = 1 - \frac{\pi cS}{4\omega V} + \frac{\pi c^2 L}{8\omega^2 V},$$
$$\gamma_{\mathrm{t}xy} = \frac{\pi c L_x L_y}{2\omega V}\left[1 - \frac{c(L_x + L_y)}{\omega L_x L_y}\right], \quad \gamma_{\mathrm{a}x} = \frac{\pi c^2 L_x}{2\omega^2 V},$$

with the total edge length $L = 4(L_x + L_y + L_z)$. Consequently, the reverberation of the total specular field is composed of seven kinds of exponential decay, arising from one oblique, three tangential, and three axial source groups. Each decay rate in decibels per unit time is given by

$$D^{\mathrm{S}}_{\mathrm{ob}(\mathrm{t}xy,\mathrm{a}x)} = 10\log_{10}e \cdot c\hat{A}_{\mathrm{ob}(\mathrm{t}xy,\mathrm{a}x)}/V, \tag{14}$$

with the relation

$$\min\left(D^{\mathrm{S}}_{\mathrm{a}x}, D^{\mathrm{S}}_{\mathrm{a}y}, D^{\mathrm{S}}_{az}\right) < \min\left(D^{\mathrm{S}}_{\mathrm{t}xy}, D^{\mathrm{S}}_{\mathrm{t}yz}, D^{\mathrm{S}}_{\mathrm{t}zx}\right) < D^{\mathrm{S}}_{\mathrm{ob}}. \tag{15}$$

Equation (13) entirely corresponds to the approximate expression derived from the normal mode theory in wave acoustics.[26,27] The critical angles for axial and tangential image sources can be interpreted in view of normal mode distribution in wavenumber space, as illustrated in Fig. 3. Supposing the ranges dominated by axial modes to be within the middle to the adjacent oblique modes, the critical angles are determined by

$$\frac{\pi}{2L_{y(z)}} = k\sin\theta_{y(z)} \approx k\theta_{y(z)}, \tag{16}$$

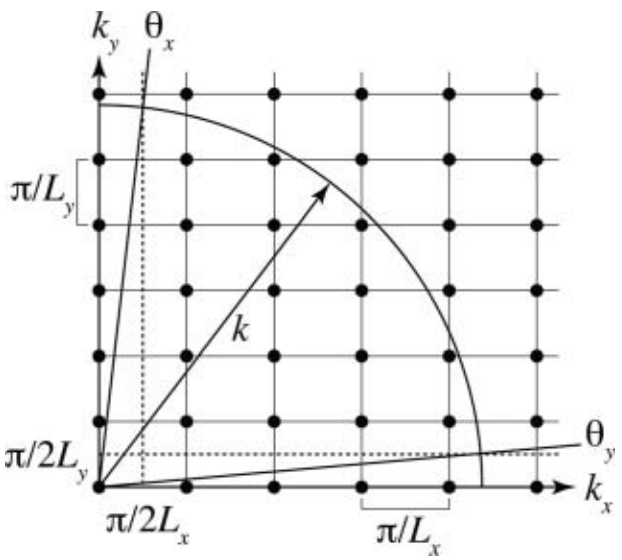

FIG. 3. Axial modes in the xy plane in wavenumber space.

which is consistent with Eq. (5). Thus it can be stated that the angular ranges for axial and tangential image sources approximately correspond to axial and tangential modes in wavenumber space.

It should be noted that the present theory includes three reasonable modifications to the original theory by Hirata,[11] on the critical angles, the averaging of absorption coefficients, and the ratios of normalization factors. In the original theory, different angular ranges were derived from an ambiguous discussion, resulting in some discrepancy with the expression based on the normal mode theory. Regarding absorption coefficients, alternate reflections between parallel walls were not considered, and arithmetic averages weighted with reflection frequency were given regardless of one- or two-dimensional field, thus finally leading to different decay rates.[28]

In the modified theory, geometric averages are used with regard to independence of reflection frequencies. However, if it is applied to extreme cases where one of the walls has perfect absorption, all of the one-dimensional fields and a two-dimensional field that is tangential to the absorptive wall vanish completely. Therefore the modified theory is not applicable to such cases, specifically with perfect absorption for grazing incidence. If the original theory is applied to the cases, none of the one- and the two-dimensional fields vanish, even a one-dimensional field that is normal to the absorptive wall. It is not realistic from a different aspect, so the original theory is also not applicable to such cases, specifically those with perfect absorption for normal incidence.

III. REVERBERATION IN RECTANGULAR ROOMS WITH SURFACE SCATTERING

A. Specular and diffuse fields with surface scattering

The scattering coefficient of a diffuse surface is defined as the ratio of nonspecularly reflected energy to total reflected energy.[18] By introducing the scattering coefficients of wall surfaces, sound energy propagating from image sources can be divided into specular and diffuse components at each reflection. One possible assumption is that the specular reflection field is composed of arriving components that are never scattered at all reflections from image sources to a receiving point. On that assumption, the energy density of the specular field is simply given by replacing all values related to absorption coefficient with those related to *specular* absorption coefficient $\beta = \alpha + (1 - \alpha)s$, with s the scattering coefficient. Accordingly, Eq. (13) is modified by substituting all kinds of $\tilde{\beta}$, β_{E}, B, and $\hat{\beta}$ for $\tilde{\alpha}$, α_{E}, A, and $\hat{A}$, as follows:

$$E^{\mathrm{S}}(t) = \frac{W}{c}\left[\frac{\gamma_{\mathrm{ob}}}{\hat{B}_{\mathrm{ob}}}\exp\left(-\frac{c\hat{B}_{\mathrm{ob}}}{V}t\right) + \sum_{xy}\frac{2\gamma_{\mathrm{t}xy}}{\hat{B}_{\mathrm{t}xy}}\exp\left(-\frac{c\hat{B}_{\mathrm{t}xy}}{V}t\right) + \sum_{x}\frac{4\gamma_{\mathrm{a}x}}{\hat{B}_{\mathrm{a}x}}\exp\left(-\frac{c\hat{B}_{\mathrm{a}x}}{V}t\right)\right], \tag{17}$$

thus each decay rate is also modified as

$$D^{\mathrm{S}}_{\mathrm{ob}(\mathrm{t}xy,\mathrm{a}x)} = 10\log_{10}e \cdot c\hat{B}_{\mathrm{ob}(\mathrm{t}xy,\mathrm{a}x)}/V. \tag{18}$$

As illustrated in Fig. 4, it is assumed that a part of the specular energy is transformed into diffuse energy at each refection, and after the transition, the diffuse energy is decayed by perfectly diffuse reflections and finally arrives to a receiving point by random incidence. With respect to an arbitrary distance r' from an image source, the rate of scattered energy in a very small path is given by

$$\lim_{dr'\to 0} 1-(1-s_{\mathrm{ob}})^{dr'/l_{\mathrm{ob}}} = \lim_{dr'\to 0} 1-\exp\left(-\frac{s_{\mathrm{Eob}}dr'}{l_{\mathrm{ob}}}\right) \to \frac{s_{\mathrm{Eob}}dr'}{l_{\mathrm{ob}}} = \frac{\hat{S}_{\mathrm{ob}}dr'}{V}, \tag{19}$$

with $\hat{S}_{\mathrm{ob}} = S_{\mathrm{ob}}/4$, $S_{\mathrm{ob}} = Ss_{\mathrm{Eob}}$, and $s_{\mathrm{Eob}} = -\ln(1 - s_{\mathrm{ob}})$. The average scattering coefficient for the three-dimensional specular field is given by

$$s_{\mathrm{ob}} = \frac{L_yL_z(1-\tilde{\alpha}^{\mathrm{r}}_x)\tilde{s}^{\mathrm{r}}_x + L_zL_r(1-\tilde{\alpha}^{\mathrm{r}}_y)\tilde{s}^{\mathrm{r}}_y + L_xL_y(1-\tilde{\alpha}^{\mathrm{r}}_z)\tilde{s}^{\mathrm{r}}_z}{L_yL_z(1-\tilde{\alpha}^{\mathrm{r}}_x) + L_zL_x(1-\tilde{\alpha}^{\mathrm{r}}_y) + L_xL_y(1-\tilde{\alpha}^{\mathrm{r}}_z)}, \tag{20}$$

where $\tilde{s}^{\mathrm{r}}_{x(y,z)}$ is the geometrical mean of random-incidence scattering coefficients of two parallel walls, considering alternate reflections by Eq. (2), and s_{ob} is assumed the arithmetic mean weighted with area and reflection coefficient for the three directions. Estimating the energy scattered at r' and decayed before and after the transition, and subsequently integrating it with respect to r' throughout the path, the energy density of the diffuse field for oblique sources is formulated as follows:

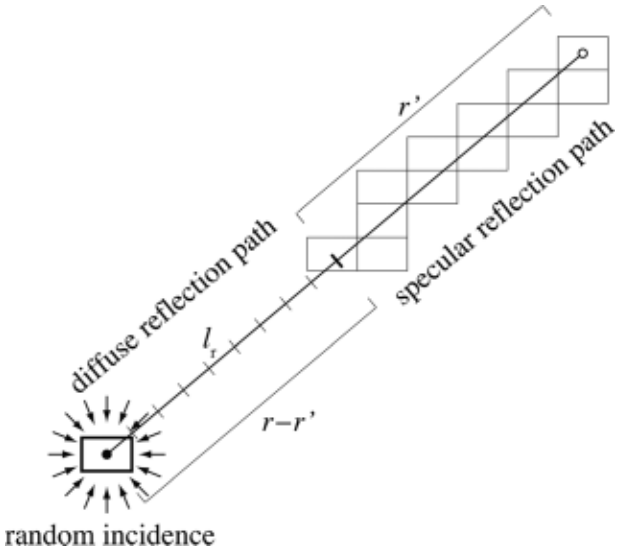

FIG. 4. Transition from specular to diffuse reflections.

$$\begin{aligned} E^{\mathrm{D}}_{\mathrm{ob}}(t) &= \frac{W}{c}\int_{ct}^{\infty}\int_0^r (1-\beta_{\mathrm{ob}})^{r'/l_{\mathrm{ob}}}(1-\alpha_{\mathrm{r}})^{(r-r')/l_{\mathrm{r}}}\frac{s_{\mathrm{Eob}}dr'}{l_{\mathrm{ob}}}\frac{dr}{V} \\ &= \frac{W}{c}\mu_{\mathrm{ob}}\int_{ct}^{\infty}[(1-\alpha_{\mathrm{r}})^{r/l_{\mathrm{r}}} - (1-\beta_{\mathrm{ob}})^{r/l_{\mathrm{ob}}}]\frac{dr}{V} \\ &= \frac{W}{c}\mu_{\mathrm{ob}}\left[\frac{1}{\hat{A}_{\mathrm{r}}}\exp\left(-\frac{c\hat{A}_{\mathrm{r}}}{V}t\right) - \frac{1}{\hat{B}_{\mathrm{ob}}}\exp\left(-\frac{c\hat{B}_{\mathrm{ob}}}{V}t\right)\right], \end{aligned} \tag{21}$$

with $\mu_{\mathrm{ob}} = \hat{S}_{\mathrm{ob}}/(\hat{B}_{\mathrm{ob}} - \hat{A}_{\mathrm{r}})$, and the mean free path for the diffuse field l_{r}. In the specular reflection path before the transition, the energy is decayed with $\hat{B}_{\mathrm{ob}} = B_{\mathrm{ob}}/4$, $B_{\mathrm{ob}} = S\beta_{\mathrm{Eob}}$, $\beta_{\mathrm{Eob}} = -\ln(1-\beta_{\mathrm{ob}}) = \alpha_{\mathrm{Eob}} + s_{\mathrm{Eob}}$, while in the diffuse reflection path after the transition, the energy is decayed with $\hat{A}_{\mathrm{r}} = A_{\mathrm{r}}/4$, $A_r = S\alpha_{\mathrm{Er}}$, $\alpha_{\mathrm{Er}} = -\ln(1-\alpha_{\mathrm{r}})$, where α_{r} is the area-weighted mean of random-incidence absorption coefficients. The relations $l_{\mathrm{ob}} \approx l_{\mathrm{r}}$ and $\alpha_{\mathrm{ob}} \geq \alpha_{\mathrm{r}}$ hold for oblique sources, thus resulting in $\hat{B}_{\mathrm{ob}} \geq \hat{A}_{\mathrm{r}}$ and $0 \leq \mu_{\mathrm{ob}} \leq 1$.

B. Diffuse fields of axial and tangential sources

Considering axial image sources as mentioned previously, and referring to Eqs. (6) and (21), the energy density of the diffuse field from x-axial sources is formulated as follows:

$$\begin{aligned} E^{\mathrm{D}}_{\mathrm{ax}}(t) &= \frac{W}{c}\int_{ct}^{\infty}\int_0^r (1-\tilde{\beta}^{\mathrm{n}}_x)^{r'/L_x}(1-\tilde{\beta}^{\mathrm{g}}_y)^{r'\theta_y/2L_y} \\ &\quad\times(1-\tilde{\beta}^{\mathrm{g}}_z)^{r'\theta_z/2L_z}(1-\alpha_{\mathrm{r}})^{(r-r')/l_{\mathrm{r}}}\frac{s_{\mathrm{Eax}}dr'}{l_x} \\ &\quad\times\frac{2(2\theta_y)(2\theta_z)dr}{4\pi V} \\ &= \frac{W}{c}\frac{\pi c^2L_x}{2\omega^2V}\int_{ct}^{\infty}\int_0^r (1-\beta_{\mathrm{ax}})^{r'/l_x}(1-\alpha_{\mathrm{r}})^{(r-r')/l_{\mathrm{r}}} \\ &\quad\times\frac{\hat{S}_{\mathrm{ax}}dr'}{V}\frac{dr}{V} \\ &= \frac{W}{c}\frac{\pi c^2L_x}{2\omega^2V}\mu_{\mathrm{ax}}\left[\frac{1}{\hat{A}_{\mathrm{r}}}\exp\left(-\frac{c\hat{A}_{\mathrm{r}}}{V}t\right)\right. \\ &\quad\left.-\frac{1}{\hat{B}_{\mathrm{ax}}}\exp\left(-\frac{c\hat{B}_{\mathrm{ax}}}{V}t\right)\right], \end{aligned} \tag{22}$$

with $\mu_{\mathrm{ax}} = \hat{S}_{\mathrm{ax}}/(\hat{B}_{\mathrm{ax}} - \hat{A}_{\mathrm{r}})$, where the contribution of axial sources to diffuse field is equal to that of oblique sources due to random incidence to the room. Regarding wall scattering, $\hat{S}_{\mathrm{ax}} = S_{\mathrm{ax}}/2$, $S_{\mathrm{ax}} = 2L_yL_zs_{\mathrm{Eax}}$, $s_{\mathrm{Eax}} = -\ln(1 - s_{\mathrm{ax}})$, and similar to Eq. (7),

$$s_{\mathrm{ax}} = 1-(1-\tilde{s}^{\mathrm{n}}_x)(1-\tilde{s}^{\mathrm{g}}_y)^{\varepsilon_{\mathrm{axy}}}(1-\tilde{s}^{\mathrm{g}}_z)^{\varepsilon_{\mathrm{axz}}}, \tag{23}$$

with $\tilde{s}^{\mathrm{n}}_x$ the normal-incidence scattering coefficient of the x-directional walls and $\tilde{s}^{\mathrm{g}}_{y(z)}$ the grazing-incidence scattering coefficients of the y- and z-directional walls, considered as the geometric mean for parallel walls according to Eq. (2). Again, because the above-presented normal- and grazing-incidence coefficients are the averages within the frequency-dependent angular range, a database of directional scattering coefficients is needed, which can be obtained by the

free field measurement[18] or numerical computation.[20] If the one-dimensional specular field decays more rapidly than the diffuse field ($\hat{B}_{ax} > \hat{A}_r$), $\mu_{ax} \geq 0$. Otherwise, the sign of the inequality is changed, where the decay of the diffuse field is obeyed by the one-dimensional specular field, and a flutter echo is liable to occur. In the singular case that $\hat{B}_{ax} = \hat{A}_r$, Eq. (22) can be transformed into

$$E^{D}_{ax}(t) = \frac{W}{c}\frac{\pi c^2 L_x}{2\omega^2 V}\frac{s_{Eax}}{\beta_{Eax}}\frac{1+\hat{A}_r ct/V}{\hat{A}_r}\exp\left(-\frac{c\hat{A}_r}{V}t\right). \quad (24)$$

Similar to absorption coefficient, it should be noted that Eq. (23) is not valid for an extreme case in which either grazing-incidence scattering coefficient $\tilde{s}^{g}_{y(z)} = 1$, because the specular component of x-axial sources perfectly vanishes in Eq. (17), even if one of the y- and z-directional walls has perfect diffusion.

In a similar way to axial sources, the energy density of the diffuse field from xy-tangential sources is formulated as follows:

$$\begin{aligned} E^{D}_{txy}(t) &= \frac{W}{c}\int_{ct}^{\infty}\int_{0}^{r}(1-\tilde{\beta}^{r}_{xy})^{r'/l_{xy}}(1-\tilde{\beta}^{g}_{z})^{r'\theta_z/2L_z} \\ &\quad\times(1-\alpha_r)^{(r-r')/l_r}\frac{s_{Etxy}dr'}{l_{xy}}\frac{2\pi(2\theta_z)dr}{4\pi V} \\ &= \frac{W}{c}\frac{\pi c L_x L_y}{2\omega V}\int_{ct}^{\infty}\int_{0}^{r}(1-\beta_{txy})^{r'/l_{xy}}(1-\alpha_r)^{(r-r')/l_r} \\ &\quad\times\frac{\hat{S}_{txy}dr'}{V}\frac{dr}{V} \\ &= \frac{W}{c}\frac{\pi c L_x L_y}{2\omega V}\mu_{txy}\left[\frac{1}{\hat{A}_r}\exp\left(-\frac{c\hat{A}_r}{V}t\right)\right. \\ &\quad\left.-\frac{1}{\hat{B}_{txy}}\exp\left(-\frac{c\hat{B}_{txy}}{V}t\right)\right], \end{aligned} \quad (25)$$

with $\mu_{txy} = \hat{S}_{txy}/(\hat{B}_{txy} - \hat{A}_r)$. Regarding wall scattering, $\hat{S}_{txy} = S_{txy}/\pi$, $S_{txy} = 2(L_x + L_y)L_z s_{Etxy}$, $s_{Etxy} = -\ln(1 - s_{txy})$, and similarly to Eqs. (10) and (11),

$$s_{txy} = 1 - (1-\tilde{s}^{r}_{xy})(1-\tilde{s}^{g}_{z})^{6_{tz}}, \quad (26)$$

$$\tilde{s}^{r}_{xy} = \frac{L_y(1-\tilde{\alpha}^{r}_{x})\tilde{s}^{r}_{x} + L_x(1-\tilde{\alpha}^{r}_{y})\tilde{s}^{r}_{y}}{L_y(1-\tilde{\alpha}^{r}_{x}) + L_x(1-\tilde{\alpha}^{r}_{y})}, \quad (27)$$

assuming the arithmetic mean weighted with area and reflection coefficient for the two directions. Again, $\mu_{txy} \geq 0$ if $\hat{B}_{txy} > \hat{A}_r$, otherwise changing the sign of the inequality. In the singular case that $\hat{B}_{txy} = \hat{A}_r$, Eq. (25) can be transformed into

TABLE I. Dimensions and absorption coefficients of rectangular rooms.

Case	L_x (m)	L_y (m)	L_z (m)	α_x	α_y	α_z	α_x/L_x: α_y/L_y: α_z/L_z
1a	10	10	10	0.35	0.35	0.35	1: 1: 1
1b	10	10	10	0.15	0.30	0.60	1: 2: 4
2a	20	10	5	0.30	0.30	0.30	1: 2: 4
2b	20	10	5	0.10	0.20	0.40	1: 4: 16

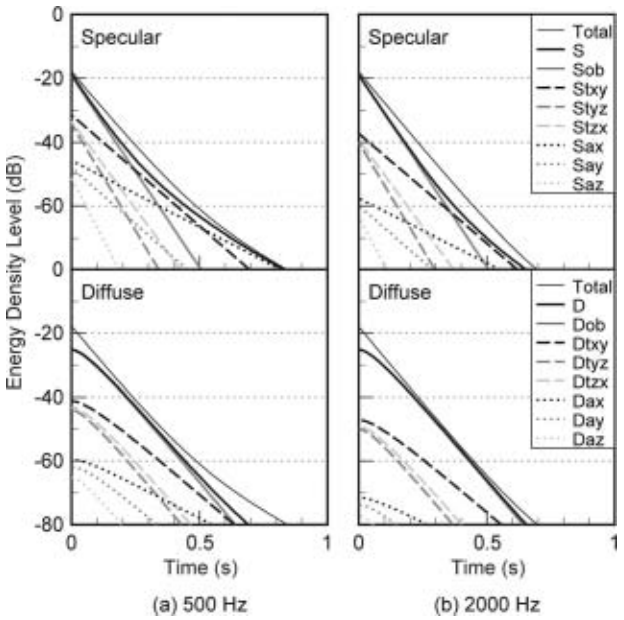

FIG. 5. Energy decay of specular, diffuse, and total fields for case 1b, with a scattering coefficient of 0.1: (a) 500 Hz, (b) 2000 Hz. Abbreviations: Specular/diffuse fields in subtotal (S/D), of oblique sources (Sob/Dob), of xy-tangential sources (Stxy/Dtxy), of x-axial sources (Sax/Dax).

$$E^{D}_{txy}(t) = \frac{W}{c}\frac{\pi c L_x L_y}{2\omega V}\frac{s_{Etxy}}{\beta_{Etxy}}\frac{1+\hat{A}_r ct/V}{\hat{A}_r}\exp\left(-\frac{c\hat{A}_r}{V}t\right). \quad (28)$$

Note that Eq. (26) is again not valid if one of the z-directional walls has perfect diffusion with yielding $\tilde{s}^{g}_{z} = 1$, because the specular component of xy-tangential sources perfectly vanishes in Eq. (17).

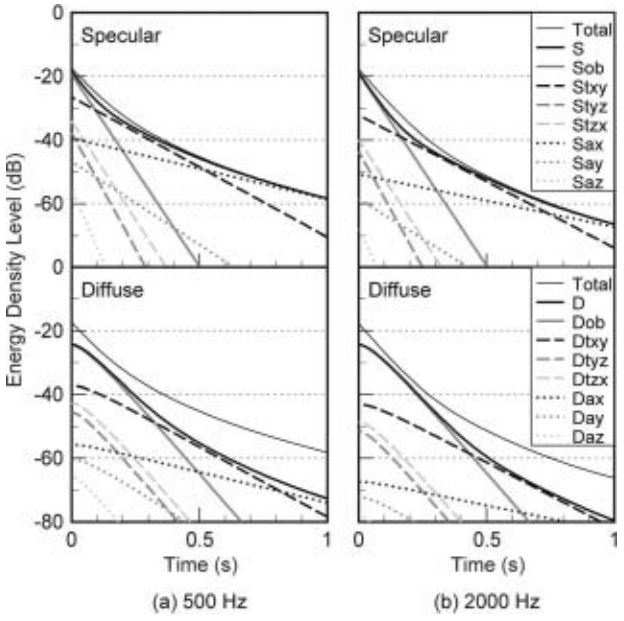

FIG. 6. Energy decay of specular, diffuse, and total fields for case 2b, with a scattering coefficient of 0.1: (a) 500 Hz, (b) 2000 Hz. Abbreviations: See Fig. 5.

C. Reverberation of total diffuse field

Similar to the total specular field, summing up Eqs. (21), (22), and (25) and excluding the duplicate contributions of axial and tangential sources, the total energy density of diffuse fields in the room is expressed by

$$E^{\mathrm{D}}(t)=\frac{W}{c}\left\{\gamma_{\mathrm{ob}}\mu_{\mathrm{ob}}\left[\frac{1}{\hat{A}_{\mathrm{r}}}\exp\left(-\frac{c\hat{A}_{\mathrm{r}}}{V}t\right)-\frac{1}{\hat{B}_{\mathrm{ob}}}\exp\left(-\frac{c\hat{B}_{\mathrm{ob}}}{V}t\right)\right]+\sum_{xy}\gamma_{\mathrm{t}xy}\mu_{\mathrm{t}xy}\left[\frac{1}{\hat{A}_{\mathrm{r}}}\exp\left(-\frac{c\hat{A}_{\mathrm{r}}}{V}t\right)-\frac{1}{\hat{B}_{\mathrm{t}xy}}\exp\left(-\frac{c\hat{B}_{\mathrm{t}xy}}{V}t\right)\right]\right.$$
$$\left.+\sum_{x}\gamma_{\mathrm{a}x}\mu_{\mathrm{a}x}\left[\frac{1}{\hat{A}_{\mathrm{r}}}\exp\left(-\frac{c\hat{A}_{\mathrm{r}}}{V}t\right)-\frac{1}{\hat{B}_{\mathrm{a}x}}\exp\left(-\frac{c\hat{B}_{\mathrm{a}x}}{V}t\right)\right]\right\}, \tag{29}$$

where $\gamma_{\mathrm{ob(t}xy,\mathrm{a}x)}$ are the proportions of sources as denoted for Eq. (13). At $t=0$, the total energy density in the steady state is expressed by

$$E^{\mathrm{D}}(0)=\frac{W}{c\hat{A}_{\mathrm{r}}}\left(\gamma_{\mathrm{ob}}\frac{s_{\mathrm{Eob}}}{\beta_{\mathrm{Eob}}}+\sum_{xy}\gamma_{\mathrm{t}xy}\frac{s_{\mathrm{Et}xy}}{\beta_{\mathrm{Et}xy}}+\sum_{x}\gamma_{\mathrm{a}x}\frac{s_{\mathrm{Ea}x}}{\beta_{\mathrm{Ea}x}}\right). \tag{30}$$

It is confirmed that if all wall surfaces are perfectly diffuse with $s\rightarrow 1$, $s_{\mathrm{E}}/\beta_{\mathrm{E}}\rightarrow 1$, thus resulting in $E^{\mathrm{D}}(0)\rightarrow W/c\hat{A}_{\mathrm{r}}$.

The reverberation of the total diffuse field is also apparently composed of seven kinds of decay, but double exponential decay. With the decay rate of the three-dimensional perfectly diffuse field, $D_{\mathrm{r}}^{\mathrm{D}}=10\log_{10}e\cdot c\hat{A}_{\mathrm{r}}/V$ each rate is given by

$$D^{\mathrm{D}}_{\mathrm{ob(t}xy,\mathrm{a}x)}(t)=D_{\mathrm{r}}^{\mathrm{D}}\frac{1-\exp[-\left(-\hat{B}_{\mathrm{ob(t}xy,\mathrm{a}x)}-\hat{A}_{\mathrm{r}}\right)ct/V]}{1-\left(\hat{A}_{\mathrm{r}}/\hat{B}_{\mathrm{ob(t}xy,\mathrm{a}x)}\right)\exp[-\left(\hat{B}_{\mathrm{ob(t}xy,\mathrm{a}x)}-\hat{A}_{\mathrm{r}}\right)ct/V]}. \tag{31}$$

In Eq. (31), just after stopping the source ($t\rightarrow 0$), $D^{\mathrm{D}}_{\mathrm{ob(t}xy,\mathrm{a}x)}(t)\rightarrow 0$; that is, all seven groups of sources do not immediately start to decay. In the late decay ($t\rightarrow\infty$), $D^{\mathrm{D}}_{\mathrm{ob}}(t)\rightarrow D_{\mathrm{r}}^{\mathrm{D}}\leq D^{\mathrm{S}}_{\mathrm{ob}}$ for oblique sources, while $D^{\mathrm{D}}_{\mathrm{t}xy(\mathrm{a}x)}(t)\rightarrow \min\left(D_{\mathrm{r}}^{\mathrm{D}},D^{\mathrm{S}}_{\mathrm{t}xy(\mathrm{a}x)}\right)$ for axial and tangential sources, where the decay rates of the specular fields $D^{\mathrm{S}}_{\mathrm{t}xy(\mathrm{a}x)}$ are given by Eq. (18).

D. Integrated reverberation in rectangular rooms

On account that specular and diffuse reflection fields are superposed, the reverberation of an actual room is generally observed as the overall energy decay. Adding the energy density of specular and diffuse fields by Eqs. (17) and (29), the overall energy density in a rectangular room is expressed by

$$E(t)=\frac{W}{c}\left[\frac{\mu_{\mathrm{r}}}{\hat{A}_{\mathrm{r}}}\exp\left(-\frac{c\hat{A}_{\mathrm{r}}}{V}t\right)+\gamma_{\mathrm{ob}}\frac{1-\mu_{\mathrm{ob}}}{\hat{B}_{\mathrm{ob}}}\exp\left(-\frac{c\hat{B}_{\mathrm{ob}}}{V}t\right)+\sum_{xy}\gamma_{\mathrm{t}xy}\frac{2-\mu_{\mathrm{t}xy}}{\hat{B}_{\mathrm{t}xy}}\exp\left(-\frac{c\hat{B}_{\mathrm{t}xy}}{V}t\right)+\sum_{x}\gamma_{\mathrm{a}x}\frac{4-\mu_{\mathrm{a}x}}{\hat{B}_{\mathrm{a}x}}\exp\left(-\frac{c\hat{B}_{\mathrm{a}x}}{V}t\right)\right], \tag{32}$$

with $\mu_{\mathrm{r}}=\gamma_{\mathrm{ob}}\mu_{\mathrm{ob}}+\sum_{xy}\gamma_{\mathrm{t}xy}\mu_{\mathrm{t}xy}+\sum_{x}\gamma_{\mathrm{a}x}\mu_{\mathrm{a}x}$.

Consequently, the reverberation of the room is apparently composed of eight kinds of exponential decay, of which decay rates correspond to seven rates for the specular fields $D^{\mathrm{S}}_{\mathrm{ob(t}xy,\mathrm{a}x)}$, and one rate for the diffuse field $D_{\mathrm{r}}^{\mathrm{D}}$. The relation by Eq. (15) holds among the former seven rates, thus the total decay rate approaches $\min\left(D_{\mathrm{r}}^{\mathrm{D}},D^{\mathrm{S}}_{\mathrm{a}x},D^{\mathrm{S}}_{\mathrm{a}y},D^{\mathrm{S}}_{\mathrm{a}z}\right)$ in the late decay.

At $t=0$, the overall energy density is expressed by

$$E(0)=\frac{W}{c\hat{A}_{\mathrm{r}}}\left[\gamma_{\mathrm{ob}}\frac{\hat{A}_{\mathrm{r}}+\hat{S}_{\mathrm{ob}}}{\hat{B}_{\mathrm{ob}}}+\sum_{xy}\gamma_{\mathrm{t}xy}\frac{2\hat{A}_{\mathrm{r}}+\hat{S}_{\mathrm{t}xy}}{\hat{B}_{\mathrm{t}xy}}+\sum_{x}\gamma_{\mathrm{a}x}\frac{4\hat{A}_{\mathrm{r}}+\hat{S}_{\mathrm{a}x}}{\hat{B}_{\mathrm{a}x}}\right]. \tag{33}$$

Considering actual rooms in the mid and high frequency range, oblique sources are usually dominant in the steady state, thus roughly giving

$$E(0) \approx \frac{W}{c\hat{A}_{\mathrm{r}}} \frac{\alpha_{\mathrm{Er}} + s_{\mathrm{Eob}}}{\beta_{\mathrm{Eob}}} \leq \frac{W}{c\hat{A}_{\mathrm{r}}}, \tag{34}$$

where the ratio of specular to diffuse field is $\alpha_{\mathrm{Er}}/s_{\mathrm{Eob}}$. Accordingly, the energy density ratio of diffuse to total field in decibels is given by

$$R^{\mathrm{D}}(0) \approx -10\log_{10}\left(1 + \frac{\alpha_{\mathrm{Er}}}{s_{\mathrm{Eob}}}\right), \tag{35}$$

which depends on the average scattering coefficient for oblique sources with the conventional average absorption coefficient. In the late decay ($t \to \infty$), if $D_{\mathrm{r}}^{\mathrm{D}}$ is the minimum rate ($\hat{A}_{\mathrm{r}} \leq \hat{B}_{\mathrm{ax}(y,z)}$), the energy of the specular field vanishes earlier than the diffuse field, thus $R^{\mathrm{D}}(t) \to 0$. Otherwise, the contribution of one of axial source groups lingers with the minimum rate among $D_{\mathrm{ax}(y,z)}^{\mathrm{S}}$, and the energy is balanced between the specular and the diffuse fields as follows:

$$R^{\mathrm{D}}(t) \to -10\log_{10}\left(1 + 4\frac{\hat{A}_{\mathrm{r}} - \hat{B}_{\mathrm{ax}(y,z)}}{\hat{S}_{\mathrm{ax}(y,z)}}\right), \tag{36}$$

which depends on the average scattering and absorption coefficients for the one-dimensional field, with the conventional average absorption coefficient.

IV. THEORETICAL CASE STUDY

A. Conditions of rectangular rooms

As a case study in rectangular rooms, the influences of room aspect ratio, absorption distribution, and surface scattering on reverberation are investigated by the present theory. As shown in Table I, four types of rooms are given, all of which have a volume of 1000 m^3 and an absorption area of 210 m^2, additionally assuming that absorption and scattering coefficients have no dependence on incidence angle, and the latter has an uniform value for all surfaces. Based on the two classical theories, Sabine's reverberation time is 0.77 s for all cases, whereas Eyring's is 0.62 s for cases 1a and 1b, and 0.65 s for cases 2a and 2b. In the following, energy density levels relative to $L_0 = 10\log_{10}(W/c)$ are calculated for the specular and the diffuse fields of axial, tangential, and oblique sources in each and subtotal, and for the total field.

B. Results and discussion

Figures 5 and 6 show the energy decay curve of each component, calculated for cases 1b and 2b with a scattering coefficient of 0.1, at 500 and 2000 Hz. It is seen that the

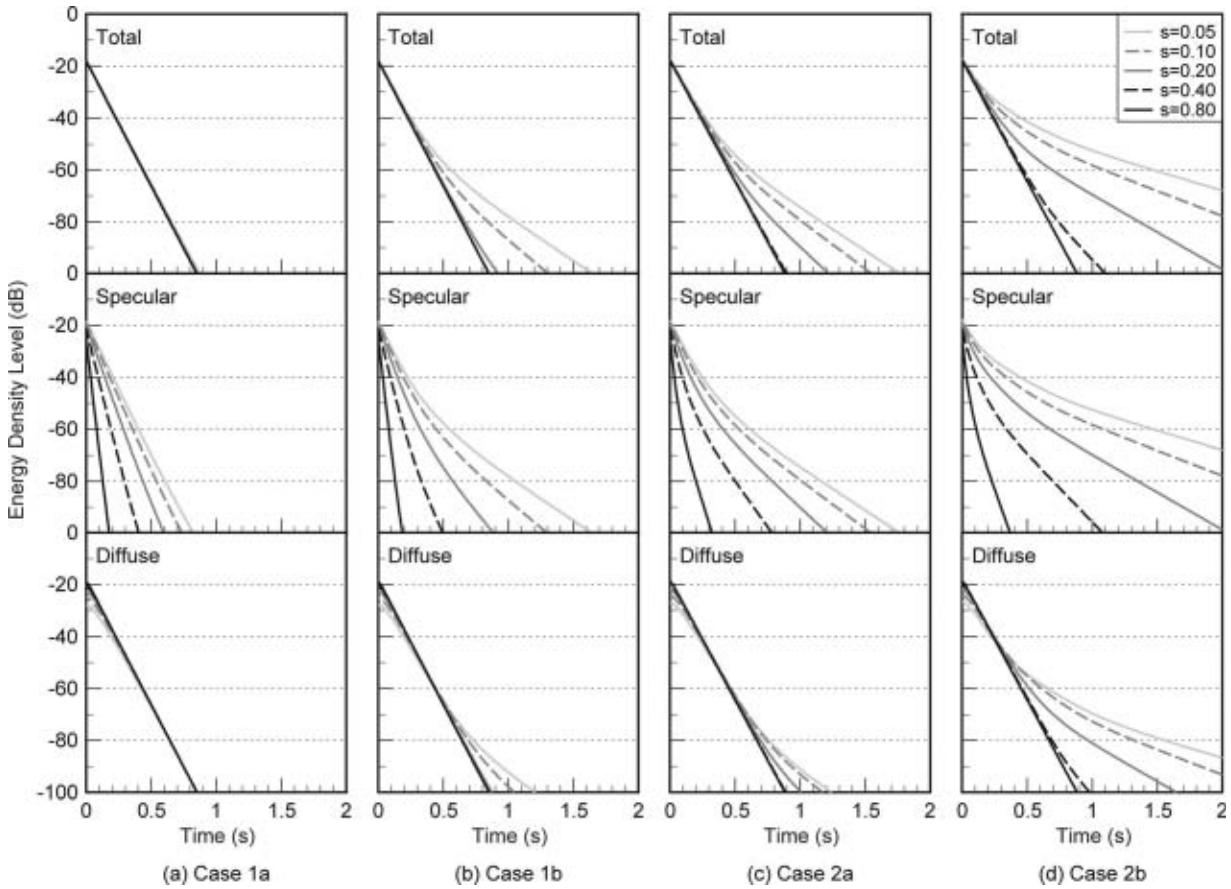

FIG. 7. Energy decay of specular, diffuse, and total fields at 500 Hz, with changing the scattering coefficient from 0.05 to 0.8: (a) Case 1a, (b) case 1b, (c) case 2a, (d) case 2b.

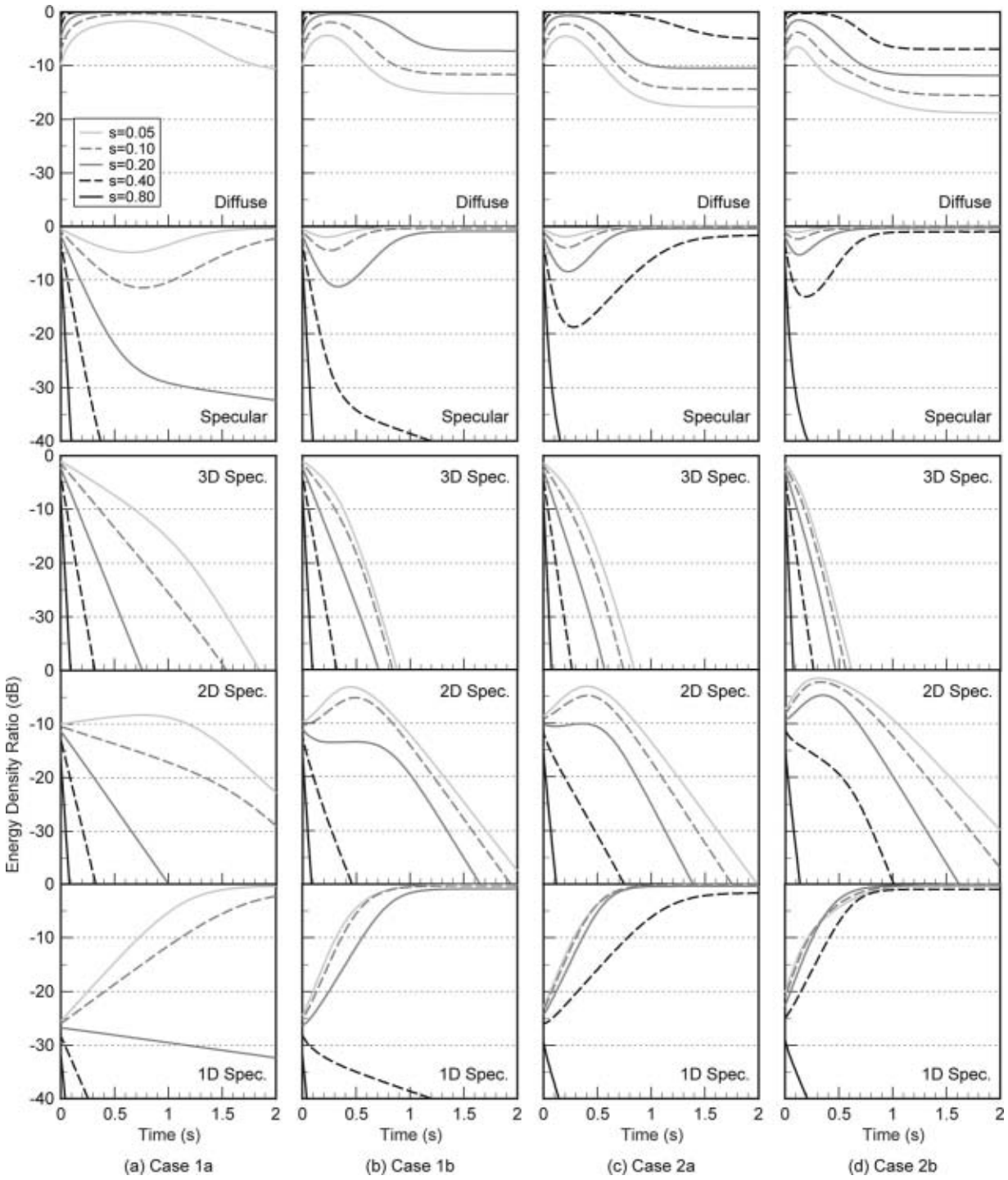

FIG. 8. Transient proportion of specular and diffuse to the total energy at 500 Hz, with changing the scattering coefficient from 0.05 to 0.8: (a) Case 1a, (b) case 1b, (c) case 2a, (d) case 2b.

decay curve of the specular field for every source group is straight, but not for the diffuse field. Regarding frequency dependence, the energy density levels of axial and tangential sources are relatively higher at the lower frequency, thus the curvature of the total decay is more remarkable, especially in case 2b.

Figure 7 shows the energy decay curves calculated at 500 Hz for all cases, uniformly changing the scattering coefficient from 0.05 to 0.8. In case 1a with cubic shape and uniform absorption, surface scattering does not affect the total decay, but it has a remarkably affect in the other cases. It is seen that with increasing the scattering coefficient the specular field decays rapidly, which suppresses the curvature of the total decay. However, the change of scattering coefficient from 0.4 to 0.8 hardly affects the total decay in all cases.

Figure 8 shows the transient proportion of specular and diffuse energy to total energy in the decay curves of Fig. 7. It is seen that at the beginning of the curves the balance between specular and diffuse energy depends on the scattering coefficient, but not on the cases under the condition of an

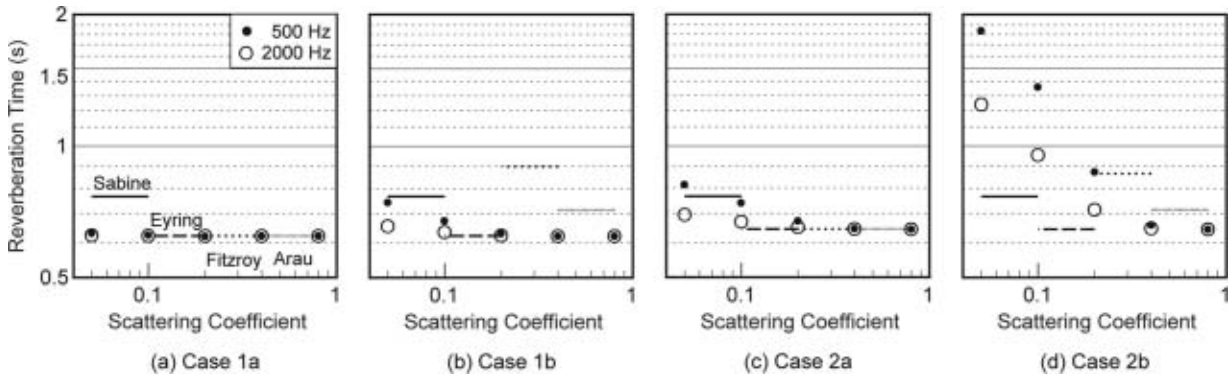

FIG. 9. Reverberation time T_{30} at 500 and 2000 Hz, with changing the scattering coefficient from 0.05 to 0.8: (a) Case 1a, (b) case 1b, (c) case 2a, (d) case 2b. Four types of lines represent theoretical values by Sabine, Eyring, Fitzroy, and Arau-Puchades.

equal absorption area. Regarding the components of the specular energy, it is observed that the three-dimensional field is dominant at the beginning, thus validating the approximation by Eq. (35). In the late decay, the ratio of diffuse energy converges to a nonzero value with increasing the ratio of one-dimensional specular energy, if the scattering coefficient is below some value that depends on the cases. This tendency can be confirmed by Eq. (36), which specifies the above-mentioned condition as $\hat{A}_{\mathrm{r}} > \hat{B}_{\mathrm{ax}}$.

Figure 9 shows the reverberation time T_{30} in the decay range from -5 to -35 dB at 500 and 2000 Hz for all cases, with changing the scattering coefficient from 0.05 to 0.8. For reference, the theoretical values by Sabine, Eyring, Fitzroy, and Arau-Puchades are indicated regardless of scattering coefficient. In all cases, the calculated values are almost equal to Eyring's if the scattering coefficient is above 0.4. On the other hand, with the lowest scattering coefficient of 0.05, increases of 5% to 30% to Eyring's are observed in cases 1b and 2a, while drastic increases of two to three times in case 2b, which are considerably beyond Fitzroy's. Up to now the present theory does not take into account additional scattering from the edges of a room, which can occur due to a difference of absorption coefficients between adjacent walls. Generally, the effect of edge scattering can be greater at lower frequencies, which will suppress reverberation of specular fields to some extent. Therefore the calculated reverberation time may be rather overestimated in rooms with very low surface scattering.

V. CONCLUSIONS

An approximate theory of reverberation in rectangular rooms with specular and diffuse reflections was newly developed based on the image source method by introducing scattering coefficients of wall surfaces. First, it was described that the specular reflection field is decomposed into one-, two-, and three-dimensional fields with frequency dependence, and its formulation corresponds to the approximate expression by the normal mode theory in wave acoustics. Second, an integrated theory for specular and diffuse fields was formulated with scattering coefficients, which expresses that the total energy decay is apparently composed of seven kinds of exponential decay for specular fields and one for the three-dimensional diffuse field. Finally, a theoretical case study demonstrated the following effects of surface scattering on energy decay in rectangular rooms: (a) With an irregular aspect ratio or nonuniform absorption distribution, the curvature of the total decay occurs if the scattering coefficient is low; (b) in the steady state, the balance between specular and diffuse energy is determined by the absorption and scattering coefficients; (c) in the late decay, the diffuse field or one of one-dimensional specular fields is dominant depending on the scattering coefficient.

However, the present theory has some problems to be further investigated for practical use. First of all, the theory is based on an approximation for specular fields that assumes single exponential decay for each group of image sources. In the strict sense, each source can have a different decay rate, which leads to a somewhat curvature in each group.[29,30] Consequently, some discrepancy from the true decay will occur in rooms with extremely irregular aspect ratio or nonuniform absorption distribution. Regarding absorption and scattering coefficients, the theory involves normal- and grazing-incidence values in addition to random-incidence values. For the normal and grazing incidence, the critical angle changes depending on the frequency and the size of a wall, which makes it troublesome to evaluate the values. A rough estimation for absorption coefficients, presented in the second section of the Appendix, may be a practical way to be tested. Furthermore, it should be noted that the theory is not applicable for an extreme case in which one of walls has perfect absorption or diffusion. A different problem may arise from the fact that the theory takes into account surface scattering on the walls, but not considering edge scattering around the walls. The influence of edge scattering should not be negligible at lower frequencies, thus some way is needed to include it.

As mentioned previously, the scope of the present theory should be intricately limited by many factors. Future work on validating the theory by experimental measurement and computational simulation, and also by comparing with other theories in various kinds of rooms is recommended.

ACKNOWLEDGMENT

This project has been funded by the Grant-in-Aid Scientific Research from Japan Society for the Promotion of Science (No. 21360275).

APPENDIX

1. Approximation of mean free paths for specular fields

Although there exist well-known arguments on the mean free path,[25,31,32] the inverse of mean reflection frequency with respect to sound speed is considered as the value for a specular field of image sources. The three-dimensional mean reflection frequency for all image sources is represented by

$$\bar{n}_{xyz} = \frac{1}{4\pi}\int_0^{2\pi}\int_0^{\pi}(n_x + n_y + n_z)\sin\theta d\theta d\varphi = \frac{cS}{4V}, \tag{A1}$$

with $n_x = c|\sin\theta\cos\varphi|/L_x$, $n_y = c|\sin\theta\sin\varphi|/L_y$, and $n_z = c|\cos\theta|/L_z$, giving the mean free path for the specular field as equal to the value for the perfectly diffuse field, $l_r = 4V/S$. By excluding axial and tangential sources, Eq. (A1) is modified for oblique sources as follows:

$$\bar{n}_{ob} = \frac{\bar{n}_{xyz} - \sum_{xy}(\bar{n}_{txy} + \bar{n}_{tz})\frac{2\pi(2\theta_z)}{4\pi} + \sum_{x}(\bar{n}_{ax} + \bar{n}_{axy} + \bar{n}_{axz})\frac{2(2\theta_y)(2\theta_z)}{4\pi}}{1 - \sum_{xy}\frac{2\pi(2\theta_z)}{4\pi} + \sum_{x}\frac{2(2\theta_y)(2\theta_z)}{4\pi}} \approx \bar{n}_{xyz}\frac{1 - \frac{2cL}{\omega S}}{1 - \frac{\pi cS}{4\omega V}}, \tag{A2}$$

with $\theta_{x(y,z)}$ the critical angles, $\bar{n}_{ax}$, $\bar{n}_{axy(z)}$ for x-axial sources, and $\bar{n}_{txy}$, $\bar{n}_{tz}$ for xy-tangential sources (see Secs. II B and II C). Thus, the mean free path for oblique sources is approximately given by

$$l_{ob} \approx \frac{4V - \pi cS/\omega}{S - 2cL/\omega} < l_r, \tag{A3}$$

for which a further approximation, $l_{ob} \approx l_r$, can be assumed for a relatively large room at mid and high frequencies.

In the same way, the two-dimensional mean reflection frequencies are modified for tangential sources except axial sources, as follows (in xy plane):

$$\bar{n}_{txy} = \frac{\bar{n}_{xy} - (\bar{n}_{ax} + \bar{n}_{axy})\frac{2\theta_y}{2\pi} - (\bar{n}_{ay} + \bar{n}_{ayx})\frac{2\theta_x}{2\pi}}{1 - \frac{2\theta_y}{2\pi} - \frac{2\theta_x}{2\pi}} \approx \bar{n}_{xy}\frac{1 - \frac{\pi c}{2\omega}\frac{1}{L_x + L_y}}{1 - \frac{c}{2\omega}\frac{L_x + L_y}{L_x L_y}}, \tag{A4}$$

with the original value, $\bar{n}_{xy} = c/l_{xy} = 2c(L_x + L_y)/\pi L_x L_y$. Thus, the mean free paths for tangential sources except axial sources are approximately given by

$$l_{txy} \approx \frac{\pi L_x L_y - \pi c(L_x + L_y)/2\omega}{2(L_x + L_y) - \pi c/\omega} < l_{xy}, \tag{A5}$$

for which a further approximation, $l_{txy} \approx l_{xy}$, can be assumed as well.

2. Estimation of normal- and grazing-incidence absorption coefficients

If local reaction is assumed on wall surfaces, the directional absorption coefficient is theoretically given by

$$\alpha_\theta = \frac{4r_n\cos\theta}{(r_n\cos\theta + 1)^2 + (x_n\cos\theta)^2}, \tag{A6}$$

where r_n and x_n are the resistance and the reactance of normalized impedance for normal incidence. With statistical averaging, the random-incidence coefficient is given by

$$\begin{aligned}\bar{\alpha}_r &= \int_0^{\pi/2}\alpha_\theta\cos\theta\sin\theta d\theta \Big/ \int_0^{\pi/2}\cos\theta\sin\theta d\theta \\ &= \frac{8r_n}{r_n^2 + x_n^2}\left\{1 + \frac{r_n^2 - x_n^2}{x_n(r_n^2 + x_n^2)}\tan^{-1}\left(\frac{x_n}{1 + r_n}\right) - \frac{r_n}{r_n^2 + x_n^2}\ln[(1 + r_n)^2 + x_n^2]\right\},\end{aligned} \tag{A7}$$

which was first derived by Paris.[33]

In the same way, limiting the incidence angles from 0 to θ_c, that is a critical angle defined by Eq. (3), the quasi-normal-incidence coefficient for the corresponding axial sources is expressed by

$$\begin{aligned}\bar{\alpha}_n = \frac{8r_n}{(r_n^2 + x_n^2)\sin^2\theta_c}\Bigg\{1 - \cos\theta_c + \frac{r_n^2 - x_n^2}{x_n(r_n^2 + x_n^2)} \times \tan^{-1}\left[\frac{x_n(1 - \cos\theta_c)}{(1 + r_n)(1 + r_n\cos\theta_c) + x_n^2\cos\theta_c}\right] \\ - \frac{r_n}{r_n^2 + x_n^2}\ln\left[\frac{(1 + r_n)^2 + x_n^2}{(1 + r_n\cos\theta_c)^2 + (x_n\cos\theta_c)^2}\right]\Bigg\}.\end{aligned} \tag{A8}$$

For a small angle of θ_c, Eq. (A8) is almost equal to the true normal-incidence coefficient,

$$\bar{\alpha}_n \approx \alpha_0 = \frac{4r_n}{(r_n + 1)^2 + x_n^2}, \tag{A9}$$

because the angle dependence is fairly weak near the normal direction in Eq. (A6). Consequently, in the present reverberation theory, true normal-incidence coefficients can be used regardless of the critical angle.

On the other hand, limiting the incidence angles from $\pi/2$–θ_c to $\pi/2$, the grazing-incidence coefficient for the corresponding axial or tangential sources is expressed by

$$\bar{\alpha}_g = \frac{8r_n}{(r_n^2+x_n^2)\sin^2\theta_c}\left\{\sin\theta_c + \frac{r_n^2-x_n^2}{x_n(r_n^2+x_n^2)}\tan^{-1}\left(\frac{x_n\sin\theta_c}{1+r_n\sin\theta_c}\right) - \frac{r_n}{r_n^2+x_n^2}\ln\left[(1+r_n\sin\theta_c)^2+(x_n\sin\theta_c)^2\right]\right\}. \quad \text{(A10)}$$

For a small angle of θ_c that satisfies $|x_n|\theta_c \ll 1 + r_n\theta_c$, Eq. (A10) is approximated by

$$\bar{\alpha}_g \approx \frac{8r_n^2}{(r_n^2+x_n^2)\theta_c^2}\left\{\frac{[2r_n+(r_n^2+x_n^2)\theta_c]\theta_c}{1+r_n\theta_c} - \ln[(1+r_n\theta_c)^2+(x_n\theta_c)^2]\right\}, \quad \text{(A11)}$$

and furthermore, if a real impedance is assumed ($x_n = 0$),

$$\bar{\alpha}_g \approx \frac{8}{r_n\theta_c}\left[1+\frac{1}{1+r_n\theta_c} - \frac{2}{r_n\theta_c}\ln(1+r_n\theta_c)\right], \quad \text{(A12)}$$

which results in $\bar{\alpha}_g \approx 8/r_n\theta_c$ for $r_n\theta_c \gg 1$, and $\bar{\alpha}_g \approx (8/3)\, r_n\theta_c - 4(r_n\theta_c)^2$ for $r_n\theta_c \ll 1$. Certainly it is difficult to evaluate a grazing-incidence coefficient that strongly depends on the critical angle, whereas Eq. (A12) may be useful for a rough estimate from a measured absorption coefficient.

[1]W. C. Sabine, *Collected Papers on Acoustics* (Harvard University Press, Cambridge, 1922), Chap. 1.
[2]C. F. Eyring, "Reverberation time in 'dead' rooms," J. Acoust. Soc. Am. **1**, 217–241 (1930).
[3]R. F. Norris, "A derivation of the reverberation formula," in *Architectural Acoustics*, edited by V. O. Knudsen (Wiley, New York, 1932), Appendix II.
[4]G. Millington, "A modified formula for reverberation," J. Acoust. Soc. Am. **4**, 69–82 (1932).
[5]W. J. Sette, "A new reverberation time formula," J. Acoust. Soc. Am. **4**, 193–210 (1933).
[6]H. Kuttruff, "Weglängverteilung und Nachhallverlauf in Räumen mit diffuse reflektierenden Wänden (Path-length distributions and reverberation processes in rooms with diffusely reflecting walls)," Acustica **23**, 238–239 (1970).
[7]H. Kuttruff, "Nachhall und effektive Absorption in Räumen mit diffuser Wandreflexion (Reverberation and effective absorption in rooms with diffuse wall reflections)," Acustica **35**, 141–153 (1976).
[8]M. C. Gomperts, "Do the classical reverberation formulae still have a right for existence?," Acustica **16**, 255–268 (1965).
[9]D. Fitzroy, "Reverberation formula which seems to be more accurate with nonuniform distribution of absorption," J. Acoust. Soc. Am. **31**, 893–897 (1959).
[10]J. Pujolle, "Nouvelle formule pour la durée de réverbération (New formula for the length of time of reverberation)," Rev. d'Acoust. **19**, 107–113 (1975).
[11]Y. Hirata, "Geometrical acoustics for rectangular rooms," Acustica **43**, 247–252 (1979).
[12]H. Arau-Puchades, "An improved reverberation formula," Acustica **65**, 163–179 (1988).
[13]E. Nilsson, "Decay processes in rooms with non-diffuse sound fields," Report No. TVBA-**1004**, Lund Institute of Technology (1992).
[14]R. O. Neubauer, "Estimation of reverberation time in rectangular rooms with non-uniformly distributed absorption using a modified Fitzroy equation," Build. Acoust. **8**, 115–137 (2001).
[15]B.-I. L. Dalenbäck, "Room acoustic prediction based on a unified treatment of diffuse and specular reflection," J. Acoust. Soc. Am. **100**, 899–909 (1996).
[16]Y. W. Lam, "The dependence of diffusion parameters in a room acoustics prediction model on auditorium sizes and shapes," J. Acoust. Soc. Am. **100**, 2193–2203 (1996).
[17]L. M. Wang and J. Rathsam, "The influence of absorption factors on the sensitivity of a virtual room's sound field to scattering coefficients," Appl. Acoust. **69**, 1249–1257 (2008).
[18]M. Vorländer and E. Mommertz, "Definition and measurement of random-incidence scattering coefficients," Appl. Acoust. **60**, 187–200 (2000).
[19]ISO 17497-1:2004: "Acoustics—Measurement of the sound scattering properties of surfaces, Part 1: Measurement of the random-incidence scattering coefficient in a reverberation room" (2004).
[20]Y. Kosaka and T. Sakuma, "Numerical examination on the scattering coefficients of architectural surfaces using the boundary element method," Acoust. Sci. & Tech. **26**, 136–144 (2005).
[21]J.-J. Embrechts, L. de Geetere, G. Vermeir, M. Vorländer, and T. Sakuma, "Calculation of the random-incidence scattering coefficients of a sine-shaped surface," Acust. Acta Acust. **92**, 593–603 (2006).
[22]W. B. Joyce, "The exact effect of surface roughness on the reverberation time of a uniformly absorbing spherical enclosure," J. Acoust. Soc. Am. **64**, 1429–1436 (1978).
[23]H. Kuttruff, "A simple iteration scheme for the computation of decay constant in enclosure with diffusely reflecting boundaries," J. Acoust. Soc. Am. **98**, 288–293 (1995).
[24]T. Hanyu, "A theoretical framework for quantitatively characterizing sound field diffusion based on scattering coefficient and absorption coefficient of walls," J. Acoust. Soc. Am. **128**, 1140–1148 (2010).
[25]C. W. Kosten, "The mean free path in room acoustics," Acustica **10**, 245–250 (1960).
[26]P. M. Morse and R. H. Bolt, "Sound waves in rooms," Rev. Mod. Phys. **16**, 69–150 (1944).
[27]M. Tohyama and S. Yoshikawa, "Approximate formula of the averaged sound energy decay curve in a rectangular reverberant room," J. Acoust. Soc. Am. **70**, 1674–1678 (1981).
[28]Y. Hirata, "Dependence of the curvature of sound decay curves and absorption distribution on room shapes," J. Sound Vib. **84**, 509–517 (1982).
[29]M. R. Schroeder, "Some new results in reverberation theory and measurement methods," in *Proceedings of the 5th International Congress on Acoustics*, G31, 1-4 (1965).
[30]F. Kawakami and K. Yamiguchi, "A systematic study of power-law decays in reverberation rooms," J. Acoust. Soc. Am. **80**, 543–554 (1986).
[31]L. Batchelder, "Reciprocal of the mean free path," J. Acoust. Soc. Am. **36**, 551–555 (1964).
[32]F. V. Hunt, "Remarks on the mean free path problem," J. Acoust. Soc. Am. **36**, 556–564 (1964).
[33]E. T. Paris, "On the coefficient of sound-absorption measured by the reverberation method," Philos. Mag. **5**, 489–497 (1928).